Measurements of the critical temperature and the critical magnetic field of the superconductor tin

F-Praktikum

Physikalisches Institut, Universität Würzburg, Am Hubland, 97074 Würzburg, Germany

Authorship notice:

This document is an edited translation of the Staatsexamsarbeit of Herrmann Betz, Universität Würzburg, 1973. Quotation marks and explicit references to this work are omitted in the text.

CONTENTS

I. HISTORICAL BACKGROUND

This historical overview follows the discussions in Refs. [2] and [11].

The liquefaction of helium in 1908 [1] and the subsequent improvement of cryostat design paved the way for the exploration of physical properties of solids at very low temperatures. In 1911 Kamerlingh Onnes studied the resistivity of pure metals and made a surprise discovery. Below ∼4 K, the resistance of a sample of distilled mercury dropped rapidly below the sensitivity limit of his measurement apparatus[2]. He named this new phenomenon "superconductivity". Subsequently, it was found that superconductivity is not rare property. It was soon realized that many metals and alloys become superconducting below a crticical (or transition) temperature (T_c). In 1993 Meissner and Ochsenfeld demonstrated that magnetic flux is expelled from the interior of a superconducting sample (*Meissner effect*). The phase transition between the normal state and the superconducting state is reversible. Based on this observation, Casimir and Gorter developed a thermodynamic description of the phase transition in 1934. By 1935, Fritz and Heinz London had established a phenomenological theory of the electrodynamics of a superconductor (*London theory*) using ideas of quantum mechanics. The theory was later extended by Pippard and independently by Ginzburg and Landau to account for a finite coherence length. A fully microscopic theory was developed by Bardeen, Cooper, and Schrieffer in 1957 (*BCS theory*). It predicts that electrons condense into a superfluid of Cooper pairs below T_c. The pairing originates from a retarded interaction between the electrons which is mediated by phonons. Bardeen, Cooper and Schrieffer received the Nobel Prize in Physics in 1972.

II. TWO PHENOMENA OF SUPERCONDUCTIVITY

A. Critical temperature T_c

At the turn of the 20th century, the conduction mechanism in metals was still controversial. Competing theories existed predicting either a freeze out of carriers (carriers are thermally activated), a finite residual resistance at low temperature (impurity scattering), or an eventual drop of the resistivity to zero as the temperature is lowered (thermally activated

scattering, e.g., by phonons). Kamerlingh Onnes was a proponent of the latter theory and thus conducted resistivity measurements on pure metals at the lowest temperatures. He felt vindicated when the resistivity of a series of metal samples dropped dramatically below a material-specific temperature which he called "critical temperature." The samples became superconducting. The critical temperature of tin is 3.722 K[2].

Residual resistance of a superconductor

Ordinary resistance measurements are not sensitive enough to determine an upper bound for the residual resistance of a superconductor. Instead, one monitors the persistent current in a superconducting ring. The time dependent current $I(t)$ in a ring of inductance L is given by

$$I(t) = I(0) \exp\left(-\frac{R}{L}t\right) \ .$$

A current $I(0)$ is induced in the sample by cooling the superconducting loop below T_c in a finite magnetic field. Next the field is removed and the current $I(t)$ is determined by measuring the trapped flux in the loop as a function of time t. The upper bound for the time constant of decay yields an estimate for the resistance R of the loop. The method was pioneered by Flimm[11], and Kamerlingh Onnes and Tuyn conducted a series of experiment in 1924 [2]. Similar experiments were performed by Collins in 1956 [4] and by Quinn and Ittner in 1962 [5]. They reported an upper bound for the specific resistivity of a superconductor of $4 \times 10^{-23}\,\Omega\cdot$cm.

B. Critical field H_c

When an external magnetic field H is applied to the superconductor, the magnetic flux is expelled from the interior of the sample (*Meissner effect*). Screening currents flow on the surface of the superconductor. The superconductivity persists up to a temperature-dependent critical field $H_c(T)$ at which the kinetic energy of the screening currents becomes larger than the pairing energy of the condensate. The temperature dependence was studied by Tuyn and Kamerlingh Onnes[2, 12]. It is described well by the empirical relationship

(*Tuyn formula*, see Fig. 1):

$$H_c(T) = H_0 \left[1 - \left(\frac{T}{T_c} \right)^2 \right] . \tag{1}$$

Considerations regarding the derivation of this formula are presented in the next section. The critical field H_0 of tin is 306 Gauss[2].

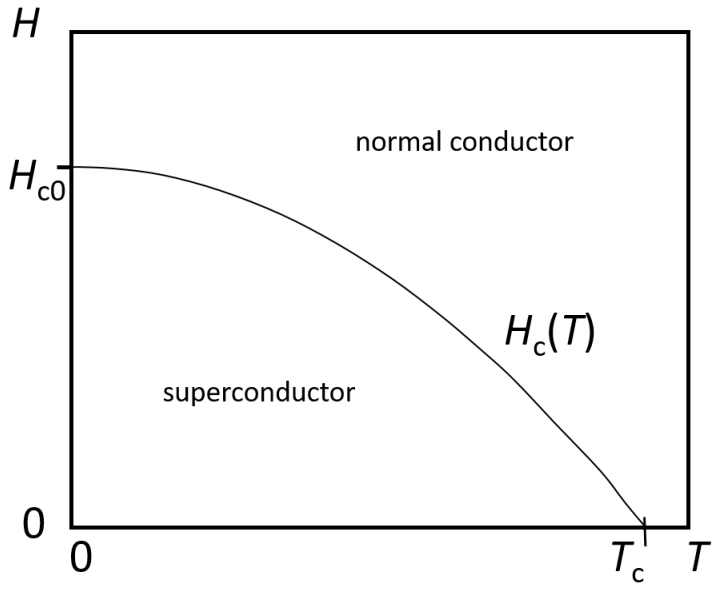

FIG. 1: Temperature dependence of the critical magnetic field H_c.

Silsbee rule

The current flow through a conductor generates a magnetic field. Thus a large current will cause the superconducting phase to break down. The current that generates a magentic field of magnitude H_c is called critical current I_c. For a cylindrical wire with radius r, the relationship[4]

$$I_c = 2\pi r H_c \, .$$

holds.

III. ELECTRODYNAMICS OF A SUPERCONDUCTOR

A. The ideal conductor

We first consider the effect of an external magnetic field $\vec{B}$ on the ideal conductor. The resistance R of an ideal conductor is zero ($R = 0$); or alternatively, its conductance σ is infinite ($\sigma = \infty$). We start from the equation of motion of and electron

$$m\dot{\vec{v}} = -e\vec{E}\,,$$

and the current density

$$\vec{j} = -ne\vec{v}\,,$$

where m and e denote the electron's mass and charge, and n is the electron density. Combining the two equations, we have

$$\dot{\vec{j}} = \frac{ne^2}{m}\vec{E}\,.$$

Let us consider the dielectric displacement $\dot{\vec{D}} \ll \vec{j}$ and the relative magnetic permeability $\mu_r = 1$. We may simplify the Maxwell equations and obtain

$$\mathrm{curl}\,\vec{B} = \mu_0\vec{j} \quad \mathrm{curl}\,\vec{E} = -\dot{\vec{B}}\,,$$

where μ_0 is the permeability of vacuum. By substiuting one euqation into the other, we have

$$\lambda^2 \mathrm{curl}\,\mathrm{curl}\,\dot{\vec{B}} = -\dot{\vec{B}}\,,$$

with $\lambda^2 = \frac{m}{\mu_0 ne^2}$. Using basic theorems of vector analysis and the Maxwell equation $\mathrm{div}\,\vec{B} = 0$, we arrive at

$$\nabla^2\dot{\vec{B}} = \frac{1}{\lambda^2}\dot{\vec{B}}\,. \tag{2}$$

Solutions of Eq. (2) for $\dot{\vec{B}}$ decay exponentially in the ideal conductor as can be easily seen for a one-dimensional geometry. Let the magnetic field $\vec{B}$ run parallel to the surface of a semi-infinite slab of an ideal conductor which fills the space $x > 0$. We may rewrite Eq. (3) for one dimension,

$$\frac{\partial^2\dot{B}}{\partial x^2} = \frac{1}{\lambda^2}\dot{B}\,,$$

with the solution

$$\dot{B}(x) = \dot{B}(0) \exp\left(-x/\lambda\right) \ ,$$

where $B(0)$ is the magnetic flux density at $x = 0$, i.e., the surface of the slab. We find that the change in magnetic flux decays exponentially in the ideal conductor. Far away from the surface, $x \gg \lambda$, we have $\dot{B} \approx 0$ and thus $B = \text{const}$. For the ideal conductor, this means that the magnetic flux density B in the interior of the material would not change from the value it had when the phase transition into the ideally conducting state occured. In other words, the phase transition would be irreversible since the final state depends on the order in which the phase transition and the ramping of the magnetic field took place, see Fig. 2.

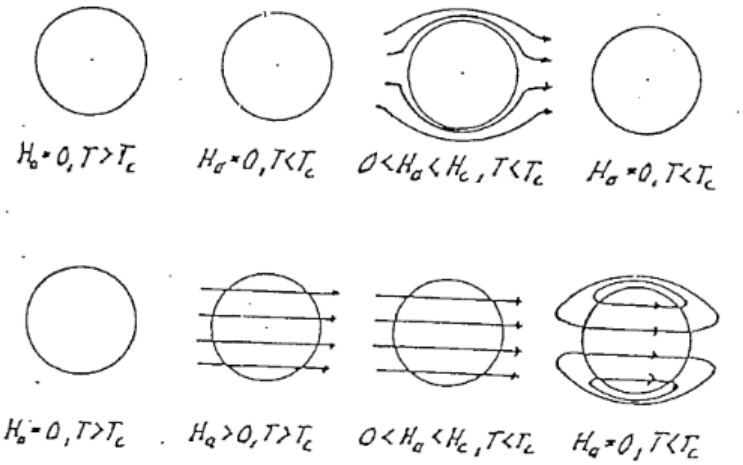

FIG. 2: Dependence of the final state of a sphere of ideal conductor on the sequence of magnetic field ramping and phase transition. Figure taken from Ref. [13]

B. Meissner-Ochsenfeld effect

In 1933, Meissner and Ochsenfeld showed that a (type-I) superconductor always expells the magnetic flux[2, 6], i.e., $\vec{B} = 0$ (deep) inside the superconductor. The phenomenon was called Meissner-Ochsenfeld effect, see Fig. 3. The final state after a superconducting transition is independent of the history of the sample in contrast to the ideal conductor. The superconducting transition is thermodynamically reversible.

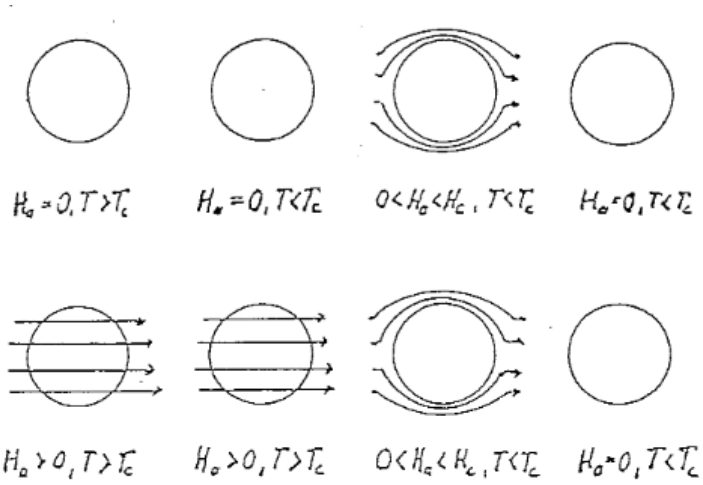

FIG. 3: Meissner-Ochsenfeld effect: The final state of a sphere of superconductor is independent of the sequence of magnetic field ramping and phase transition. Figure taken from Ref. [13].

C. London equation for the superconductor

Fritz and Heinz London suggested to add two additional equations to the Maxwell equations to describe the electrodynamics of superconductors[2]:

$$\vec{B} = -\frac{m}{ne^2}\mathrm{curl}\,\vec{j}\,,$$

and

$$\dot{\vec{j}} = \frac{ne^2}{m}\vec{E}\,.$$

Using the same steps as in the calculation for the ideal conductor (D.I.Y.), we find that Eq. (2) is replaced by

$$\nabla^2\vec{B} = \frac{1}{\lambda_L^2}\vec{B}\,. \tag{3}$$

Solutions to Eq. (3) show that both, $\dot{\vec{B}}$ as well as $\vec{B}$, decay exponentially in the superconductor. For the one-dimensional example of a semi-infinte slab of superconductor in a parallel magnetic field, we have

$$\frac{\partial^2 B}{\partial x^2} = \frac{1}{\lambda_L^2}B\,,$$

with the solution

$$B(x) = B(0)\exp\left(-x/\lambda_L\right)\,.$$

For large $x \gg \lambda_L$, we have $B \approx 0$, i.e., the magnetic flux is expelled from the interior of the superconductor. The magnetic flux density decays by a factor $1/e$ over a distance λ_L which is called the *London penetration depth*:

$$\lambda_L = \sqrt{\frac{m}{\mu_0 n e^2}}\,. \tag{4}$$

Let us now use the simplified Maxwell equation $\operatorname{curl} \vec{B} = \mu_0 \vec{j}$ and write

$$-\frac{\partial B}{\partial x} = \mu_0 j_y\,.$$

We may recast the solution for $B(x)$ into

$$j_y = \frac{B(0)}{\mu_0 \lambda_L} \exp(-x/\lambda_L) = j(0) \exp(-x/\lambda_L)\,. \tag{5}$$

Equation 5 describes surface currents that screen the magnetic flux from the interior of the superconductor. The screening currents flow close to the surface of the superconductor within a distance comparable to the London penetration depth λ_L. In experiments, it is often found that the penetration depth is much larger than the predicted value by London theory[2].

D. 'Ideal' diamagnetism

In the following, we simplify our considerations by disregarding the finite length of the London penetration depth, i.e., $\lambda_L \equiv 0$. Let us look at a superconductor in the presence of an external magnetic field $\vec{H}_a$ as a body with an internal magnetic field $\vec{H}_i$ and a magnetization $\vec{M}$. Inside the superconductor, we thus have $\vec{B}_i = 0$, $\vec{M} \neq 0$ and $\vec{H}_i \neq 0$. Here the index i denotes the inside of the superconductor.

For the magnetization of the sample, we have

$$\vec{M} = \chi \vec{H}_i\,,$$

where χ denotes the *magnetic susceptibility*. With

$$\vec{B}_i = \mu_0(\vec{H}_i + \vec{M})\,,$$

we define the *magnetic permeability* μ_r:

$$\vec{B}_i = \mu_0(1+\chi)\vec{H}_i = \mu_0\mu_r\vec{H}_i\,.$$

Since $\vec{B}_i = 0$ inside as superconductor, $\mu_r = 0$, and the superconductor can be considered an ideal diamagnet with susceptibility $\chi = -1$.

1. *Sample geometry and demagnetization factor*

Next we need to find the relationship between the externally applied magnetic field H_a and the field strength inside the superconductor H_i. For simplicity, we only consider samples in the shape of ellipsoids of revolution with the external field aligned parallel to the principal axis. In this case, B_i, H_i and M are all constant inside the superconductor and parallel to H_a. Again, we may disregard the finite penetration depth which is a good approximation if all sample dimensions are large compared to λ_L. We have [4]

$$H_i = H_a - nM\,, \tag{6}$$

where n is the *demagnetizing factor*. With $M = -H_i$, we rewrite Eq. (6) and find

$$H_i = \frac{1}{1-n}H_a\,.$$

For an ellipsoid of revolution the demagnetization factor is given by [4]

$$n = \left(\frac{1}{e^2} - 1\right)\left(\frac{1}{2e}\ln\frac{1+e}{1-e} - 1\right)\,, \tag{7}$$

where e denotes the excentricity $e = \sqrt{(1-a^2/b^2)}$, and a and b are the semimajor and semiminor axis, respectively. In the case of a sphere, $a = b$, we obtain $n = 1/3$. In the opposite limit of an infinitely long cylinder with the cylinder axis parallel to H_a, $a \gg b$, and

$n = 0$; see Fig. 4.

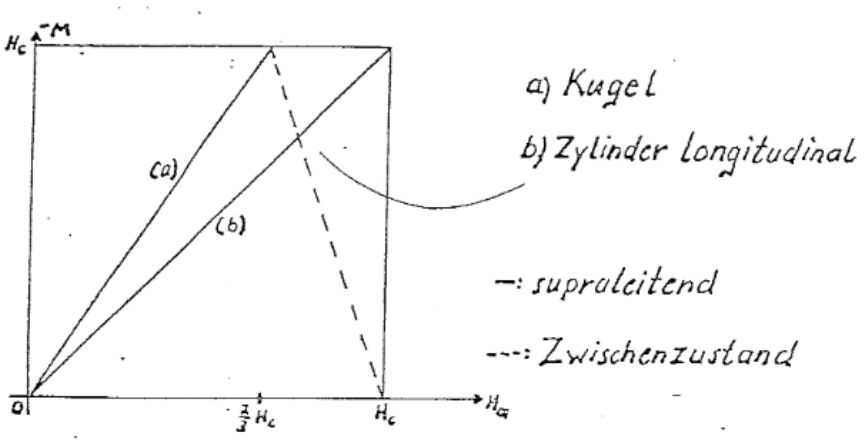

FIG. 4: Magnetization curves for a sphere (a) and long cylinder (field parallel to the cylinder axis) (b). The mixed state is indicated by the dashed line. Figure taken from Ref. [13].

2. Mixed state

Since $n = 0$ for a long cylinder, $H_i = H_a$. Hence, if the externally applied field surpasses the critical magnetic field H_c of the superconducting material, the sample will uniformly transition into the normal state. We will take advantage of this in designing our experiment by chosing a wire geometry for our sample.

For samples of general shape, $n \neq 0$, and the situation becomes more complicated. Let us revisit the ellipsoids of rotation. When applying a magnetic field $H_a < H_c$, the magnetization of the sample distorts the magnetic field. At the equator, we have [2]

$$H_{\text{equ}} = H_i = \frac{1}{1-n} H_a \,,$$

from the boundary condition for the magnetic field and at the pole

$$H_{\text{pole}} = \frac{B_i}{\mu_0} = 0 \,.$$

At an externally applied field of $H_a = (1-n)H_c$, the field at the equator of the sample reaches the critical field $H_i(\text{“equator”}) = H_c$. Thus the equator region will transition into the normal state, while $H_i < H_c$ elsewhere. In 1936 Peierls and London[2] proposed that for $H_a \geq (1 -$

$n)H_c$ normal regions with $B_i = \mu_0 H_c$ will form and other regions will remain superconducting ($B_i = 0$). Hence—as H_a increases—larger and larger regions of the superconductor will transition into the normal state, but the magnetic flux density remains $B_i = \mu_0 H_c$ at the equator.

For $(1 - n)H_c \leq H_a < H_c$, the magnetization is given by

$$M = -\frac{1}{n}(H_c - H_a)\,,$$

and the superconductor is in a *mixed state*, i.e., some regions are superconducting while others have transitioned into the normal state minimizing the free energy of the sample for a given applied magnetic field, see Fig. 5.

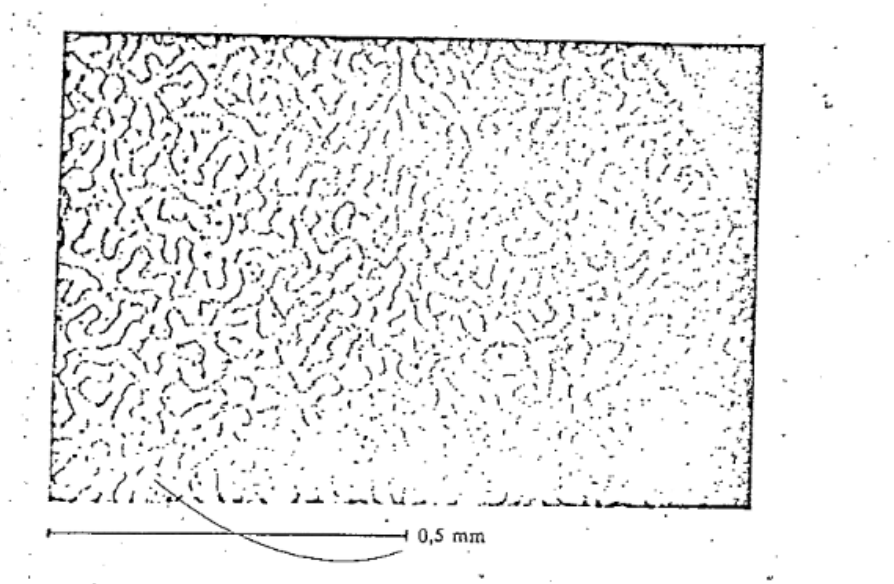

Abb. 70. Zwischenzustandsstruktur mit Hilfe des Faraday-Effektes aufgenommen. Pb-Schicht 7 μm dick, magnetooptisch aktive Schicht aus EuS und EuF_2 ca. 1000 Å dick, Magnetfeld $B \approx 0{,}77\ B_c$ senkrecht zur Schicht. Die dunklen Stellen entsprechen supraleitenden Bereichen (Wiedergabe mit freundlicher Genehmigung von Herrn Kirchner, Forschungslabor der Fa. Siemens, München).

FIG. 5: Faraday effect image of the mixed state of a 7 μm thick layer of lead at an applied magnetic field $H = 0.77\ H_c$. Figure reproduced from Ref. [13], originally from Ref. [1].

IV. THERMODYNAMIC CONSIDERATIONS

A. Gibbs free energy (free enthalpy)

First thermodynamic considerations regarding the superconducting state go back to Keesom (1924) and Rutgers and Ehrenfest (1933)[2]. However, it remained a point of debate whether the superconducting transition was indeed (thermodynamically) reversible. Following the experiments by Meissner and Ochsenfeld that established reversibility, Gorter and Casimir developed a thermodynamic description of the superconducting state in 1934[2].

Let $G_s(T, 0)$ be the Gibbs free energy of the sample in the superconducting state at temperature T and magnetic field $H = 0$. The Gibbs free energy in the normal state is denoted by $G_n(T, 0)$ for the same parameters. Considering the ideal diamagnetism of the superconductor, we define

$$G_s(T, H_0) = G_s(T, 0) - \int_V \mathrm{d}V' \int_0^{H_0} \mathrm{d}H \mu_0 M(H)\,,$$

where the second term represents the work the applied field performs on the superconductor. This work is done on the superconducting regions only, hence

$$G_s(T, H_c) = G_s(T, 0) + V\frac{\mu_0 H_c^2}{2}\,. \tag{8}$$

In the normal state, we have $\mu_r = 1$ and $\chi = 0$. For the Gibbs free energy, we may thus assume $G_n(T, H_c) = G_n(T, 0)$. Gorter and Casimir require that the Gibbs free energies are equal when the normal and superconducting phases are in equilibrium. From this follows the equilibrium condition at the critical magnetic field H_c,

$$G_s(T, H_c) = G_n(T, H_c)\,.$$

Using Eq. (8), we obtain

$$G_n(T, 0) - G_s(T, 0) = V\frac{\mu_0 H_c^2}{2} \tag{9}$$

for the difference in Gibbs free energy between the normal and the superconducting state. We rewrite this equation and find for the temperature dependence of the critical magnetic

field

$$H_c(T) = \sqrt{\frac{2}{\mu_0 V}\left[G_n(T,0) - G_s(T,0)\right]}\,.$$

B. Entropy of the phase transition

We use the thermodynamic relation

$$S = -\left[\frac{\partial G}{\partial T}\right]_{H,p}$$

to obtain the entropy of the system. Here the pressure p and the field H are held constant. We have

$$\left[\frac{\partial G_n(T,0)}{\partial T}\right]_{H,p} - \left[\frac{\partial G_s(T,0)}{\partial T}\right]_{H,p} = V\mu_0 H_c \left[\frac{\partial H_c}{\partial T}\right]_{H,p},$$

or, for the difference in entropy between the normal and the superconducting state,

$$S_n - S_s = -V\mu_0 H_c \left[\frac{\partial H_c}{\partial T}\right]_{H,p}. \tag{10}$$

First, let us consider the limit $T \to T_c$, and thus $H_c \to 0$. In this case, the difference in entropy $S_n - S_s \to 0$, i.e., the entropy of the normal state and superconducting states are equal at T_c (in the absence of an external magnetic field). In the intermediate regime, $0 \leq T < T_c$, we have $H_c > 0$ and $\partial H_c/\partial T < 0$. Hence the entropy difference is negative. The entropy of the superconducting phase is smaller than the entropy of the normal state, and the superconducting state posseses a higher degree of order. Finally, the Nernst theorem ("third law of thermodynamics") dictates that the entropy vanishes at $T = 0$. Consequently, $(S_n - S_s)(T = 0) = 0$. It is evident that the entropy difference $\Delta S = S_n - S_s$ must possess an extremal value in the range $0 < T < T_c$, see Fig. 6.

Let us revisit the formula of Tuyn, Eq. (1), for a moment. A general polynomial ansatz for the temperature dependence of H_c reads

$$H(T) = H_0\left[1 - \sum_{n=1}^{N} a_n \left(\frac{T}{T_c}\right)^n\right].$$

Following the discussion above, it becomes clear why the coefficient a_1 must be zero. If this was not the case, Nernst theorem would be violated, see Eq. (10) for $T \to 0$.

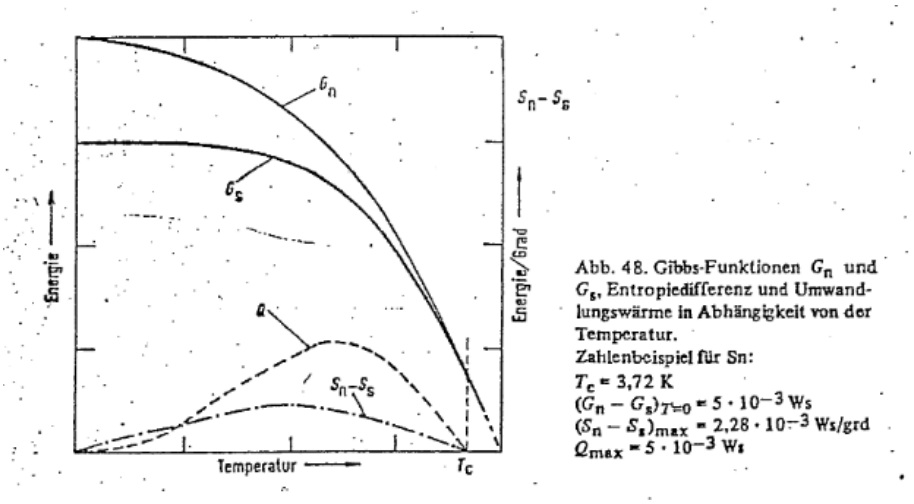

FIG. 6: Gibbs free energy of normal and superconducting states and entropy difference. Figure reproduced from Ref. [13], originally from Ref. [1].

C. Specific heat

To conclude our discussion of the thermodynamic properties of the superconductor, we take a look at the specific heat. The specific heat is obtained using the thermodynamic relation [4]

$$C = T\frac{\partial S}{\partial T}\,.$$

By differentiating Eq. (10) and multiplying by T (D.I.Y.), we find

$$C_s - C_n = TV\mu_0\left[\left(\frac{\partial H_c}{\partial T}\right)^2_{H,p} + H_c\left(\frac{\partial^2 H_c}{\partial T^2}\right)_{H,p}\right]\,. \tag{11}$$

At $T = T_c$ and $H_c = 0$ the equation simplifies to

$$C_s - C_n\Big|_{T=T_c} = T_c V\mu_0\left(\frac{\partial H_c}{\partial T}\right)^2_{H,p,T=T_c}\,. \tag{12}$$

Equation 12 is known by the name *Rutgers formula*[1]. It predicts a jump in the specific heat at $T = T_c$ since $C_s > C_n$ there, see Fig. 7. As the temperature is lowered, C_s drops faster, and it becomes equal to C_n where the entropy difference has its maximum. In the limit $T \to 0$, the specific heats of both phases vanish ($C_s, C_n \to 0$) [2].

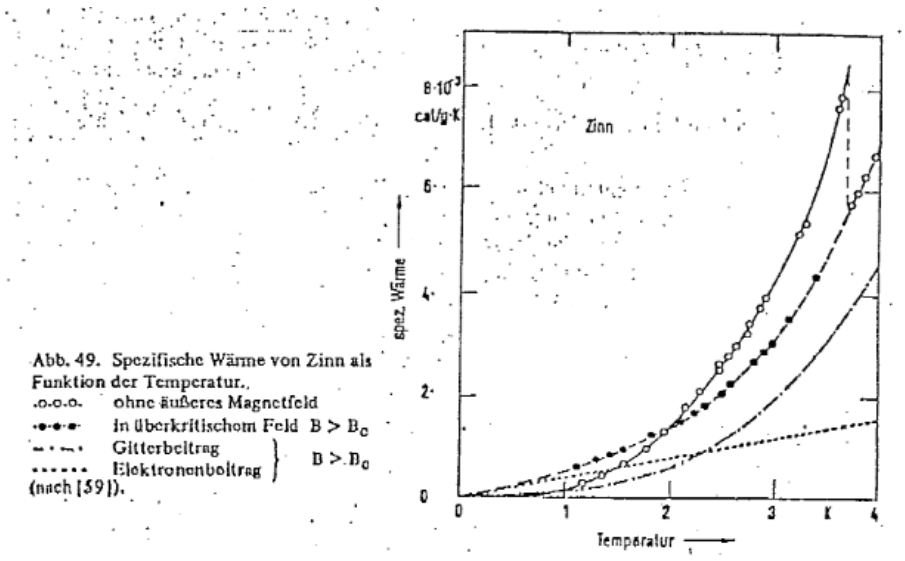

FIG. 7: Specific heat of the normal (closed circles, with magnetic field) and the superconducting state(open circles). The tin sample was driven normal by an applied magnetic field. Figure reproduced from Ref. [13], originally from Ref. [1].

V. SEMICLASSICAL THEORIES

A. Temperature dependence of the penetration depth

London theory predicts that the magnetic field penetrates into the superconductor on the characteristic length scale of the London penetration depth

$$\lambda = \sqrt{\frac{m}{\mu_0 n e^2}}\,.$$

In order to find an expression for the temperature dependence of the penetration depth, Gorter and Casimir assumed that the density of superconducting electrons varies with temperature according to [2]

$$n(T) = n_0 W(T)\,,$$

where $W(T)$ is the order parameter of the superconducting phase and n_0 is the electron density at $T = 0$. For the temperature-dependence of the order parameter, Gorter and Casimir assumed the expression [2]

$$W(T) = 1 - \left(\frac{T}{T_c}\right)^4 .$$

Substituting this into the expression for the penetration yields

$$\lambda(T) = \lambda(0) \left[1 - \left(\frac{T}{T_c} \right)^4 \right]^{-1/2} , \tag{13}$$

where $\lambda(0)$ is given by the expression for the London penetration depth with $n = n_0$. The penetration depth $\lambda(0)$ of tin is 51 nm [1].

The penetration depth also depends on the magnitude of the magnetic field and the impurity scattering in the material. Pippard described these effects by modifying local London electrodynamics to include a finite correlation length for the electron correlations.

B. Type-I and type-II superconductors, Ginzburg-Landau theory

Ginzburg and Landau developed a theory of the superconducting state based on Landau's theory of phase transitions. The order parameter of the system is chosen to be the macroscopic wave function of the superconducting condensate. The condensation energy is taken into consideration by adding terms proportional to powers of the order parameter that allow for a phenomenological description of the phase transition. Thus the theory is valid in regimes for which the order parameter is small, i.e., in large magnetic fields or close to T_c. In the context of the formalism, Ginzburg and Landau introduced a new characteristic length scale, the Ginzburg-Landau coherence length ξ_{GL}. It describes the characteristic distance for changes in the density of the superconducting condensate for a given strength of the superconducting interaction. In the presence of a magnetic field, two effects compete: Meissner screening increases the (kinetic) energy of the condensate, whereas creating a normal domain in the superconductor lowers the energy of the magnetic field distribution at the cost of losing the (negative) contribution of the condensation energy in the normal region. The Ginzburg-Landau parameter (cp. Ref. [1]),

$$\kappa = \frac{\lambda}{\xi_{GL}} , \tag{14}$$

thus serves as a criterion to distinguish two types of superconductors, type-I and type-II. Type-II superconductors are characterized by a negative surface energy, i.e., the superconductor can lower the free energy by admitting flux into the bulk of the sample and creating

normal state domains. As a consequence, type-II supercondcutors exhibit full Meissner screening only up to the critical field $H_{c1} < H_c$. Beyond this value, flux penetrates into the sample, and the magnetization reduces, see Fig. 8. The magnetization remains finite up to the upper critical field $H_{c2} > H_c$. Here H_c denotes the thermodynamic critical field, cp. Eq. (8). In the limit $\kappa \gg 1$, the critical fields can be expressed in terms of H_c [2]:

$$H_{c1} = \frac{1}{\sqrt{2}\kappa}(\ln \kappa + 0.08) H_c \,,$$

and

$$H_{c2} = \sqrt{2}\kappa H_c \,.$$

We may distinguish the two types of superconductors by requiring $H_{c2} \geq H_c$ for the type-II superconductor[1]. We define

$$\begin{aligned} \text{type} - \text{I superconductor}: &\quad \kappa < 1/\sqrt{2} \,, \\ \text{type} - \text{II superconductor}: &\quad \kappa > 1/\sqrt{2} \,. \end{aligned}$$

Tin is a type-I superconductor.

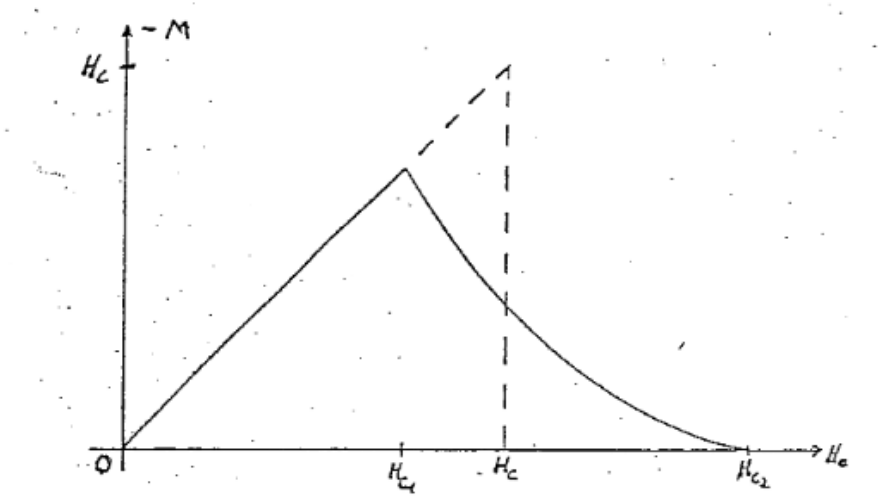

FIG. 8: Magnetization curves of a type-I (dashed line) and a type-II superconductor (solid line). Figure reproduced from Ref. [13].

1. *Isotope effect*

First studies of the effect of the atomic mass on superconductivity were attempted by Kamerlingh Onnes in 1922[1], but his experiments lacked the resolution to find a correlation. In 1950, Maxwell[2, 8], and independently Reynolds *et al.*[2, 8, 9] observed that the critical temperature T_c of mercury isotopes varies with isotope mass M according to the relation

$$T_c M^{\alpha} = \text{const.}$$

where $\alpha \approx 1/2$.

The critical temperature decreases with increasing isotope mass, and for non-transition metals, $\alpha \approx 1/2$ holds. However, exceptions exist. E.g., a measurement of Finnemore and Mapother[2, 10] showed $\alpha < 0.05$ for ruthenium isotopes. An opposite extreme is the heavy element uranium with $\alpha = -2.2$ [1]. For uranium T_c increases with isotope mass.

As the critical magnetic field H_c depends on the transition temperature, cp. Eq. (1), it is reasonable to assume a dependence of H_c on the isotope mass. In 1951 Lock *et al.*[2] found that the critical field of tin is described by the approximation

$$H_c(T) = H_0 \left[1 - 1.0720 \left(\frac{T}{T_c} \right)^2 - 0.0944 \left(\frac{T}{T_c} \right)^4 + 0.3325 \left(\frac{T}{T_c} \right)^6 - 0.1660 \left(\frac{T}{T_c} \right)^8 \right] .$$

The discovery of the isotope effect was an important step towards a theoretical description of superconductivity. Before 1950, only properties of the electronic system were considered. The observation of an isotope effect suggests that lattice vibrations play a role since the isotope mass only influences the phonon spectrum. Bardeen and Frölich independently realized that phonons can mediate a retarded, attractive interaction between electrons. This ideas became the foundation of a microscopic description of superconductivity.

VI. SOME COMMENTS ON BCS THEORY

In 1956/57, John Bardeen, Leon Cooper, and Robert Schrieffer developed a microscopic theory of superconductivity which is best-known by the three letter acronym 'BCS' theory. BCS theory is based on the idea that lattice atoms mediate a retarded interaction between the electrons: Electrons that move through the lattice polarize it locally, i.e., they move

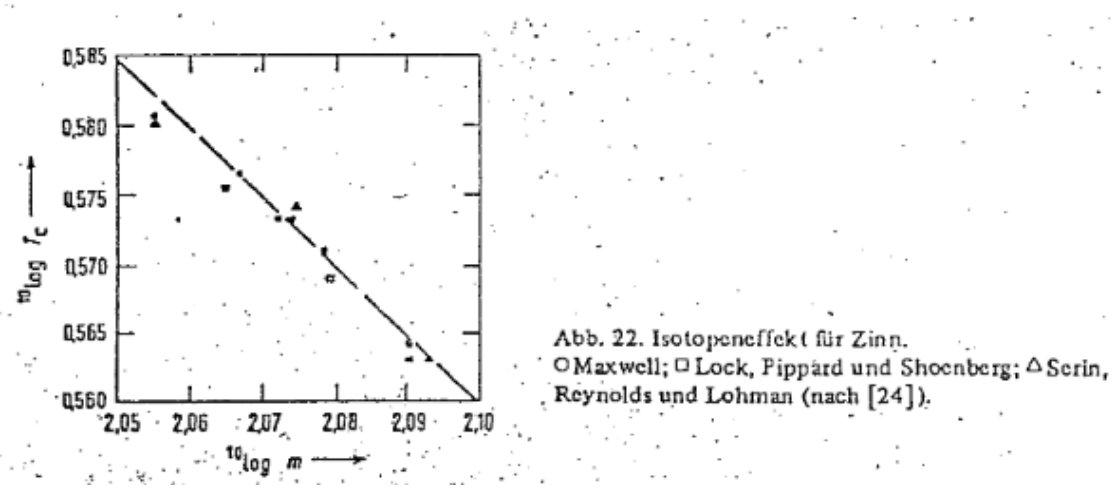

FIG. 9: Isotope effect for tin. Figure reproduced from Ref. [13], originally from Ref. [1].

the positively charged atoms away from their equilibrium positions in the lattice and thus cause lattice vibrations. When another electron travels through the lattice, it feels the finite polarization. The interaction is retarded, i.e., the interacting electrons are not in the same place. This avoids the problem of Coulomb repulsion since both electrons carry negative charge. Cooper calculated that the Fermi sea is unstable in the presence of a small, attractive interaction between the electrons. The electronic system can lower its total energy by forming *Cooper pairs* of electrons with opposite momentum and spin $\{p\uparrow, -p\downarrow\}$. All pairs are in a single, coherent quantum-mechanical state. In an electric field, all pairs acquire the same velocity and have the same kinetic energy. As a consequence, no individual pair interacts with the lattice. The pairs form a superfluid, and electric transport is frictionless (zero resistance). However, there are limits to the stability of Cooper pairs. For instance, if a large electric field is applied, the kinetic energy of the electrons becomes larger than the pairing energy. The Cooper pairs break up, and a transition into the normal state occurs.

Selected properties of the Cooper pairs:

- All Cooper pairs populate a single, coherent quantum state.
- There is an *energy gap* in the spectrum, i.e., we need to supply a finite energy 2Δ to break up a Cooper pair and create a (quasi-particle) excitation. Here, Δ denotes the pairing potential which relates to the condensation energy of the Cooper pair. The energy gap is observed in the exponential decrease of the specific heat with temperature,

in microwave absorption and ultrasonic attenuation experiments, and in tunneling conductance measurements.

- The characteristic distance ξ between the electrons that form a Cooper pair (BCS coherence length, correlation length) is $\xi \sim 0.1 - 1\,\mu$m.

- Only a fraction $\Delta/E_F \sim 1/1000$ of the electrons form Cooper pairs, where E_F is the Fermi energy.

- There are $10^6 - 10^7$ Cooper pairs in a volume $\sim \xi^3$.

VII. CRYOGENICS

The superconducting transition temperature of tin is below 4.2 K, the boiling point of liquid helium at ambient pressure. The student needs to familiarize themselves with standard methods of cooling and low temperature physics: Liquefaction of gases and properties of cryogens, evaporative cooling (pumping on liquid helium), and thermometry at low temperatures (esp. helium thermometer, ITS-90, secondary thermometers). Below we address a selection of aspects relevant for our experiment.

A. Cryostat

Liquid helium has a small latent heat. It is essential to thermally isolate the helium bath from the warm environment. For this purpose, we use a *cryostat*. The cryostat is designed to suppress heat transport (i.e., thermal conduction, convection, and radiation). This is achieved by an alternating sequence of vacuum isolation spaces and cryogenic baths. A schematic of a modern cryostat is shown in Fig. 10. The vacuum chambers are made from a material of low thermal conductivity (steel, glass, etc.). Instead of additional cryogenic baths, some modern cryostats use thin plastic foils with reflective coatings ('superinsulation') to reduce heat input from thermal radiation.

B. Variable temperature insert

Some cryostats are fitted with a *variable temperature insert* (VTI), similar to a *flow-through cryostat*. It comprises a separate vacuum-isolated space, a needle valve mechanism for introducing a well-defined, steady flow of liquid helium from the helium bath of the cryostat, and a heater. The VTI is connected to a helium pumping system to extract the helium vapor. The temperature of the VTI sample space is set by adjusting the helium flow, heater power and the pumping speed. For operation above 4.2 K, the He liquid is evaporated and the sample is cooled by the He vapor.

In the experiment, we use a 'home-made' VTI that integrates the sample stick (which holds the sample and a carbon resistor thermometer) in the mechanism for the needle valve. The VTI is placed inside a copper coil that is used to apply a magnetic field to the sample. Detailed information about the design and operation of the VTI will be provided in a short introduction at the beginning of the lab section.

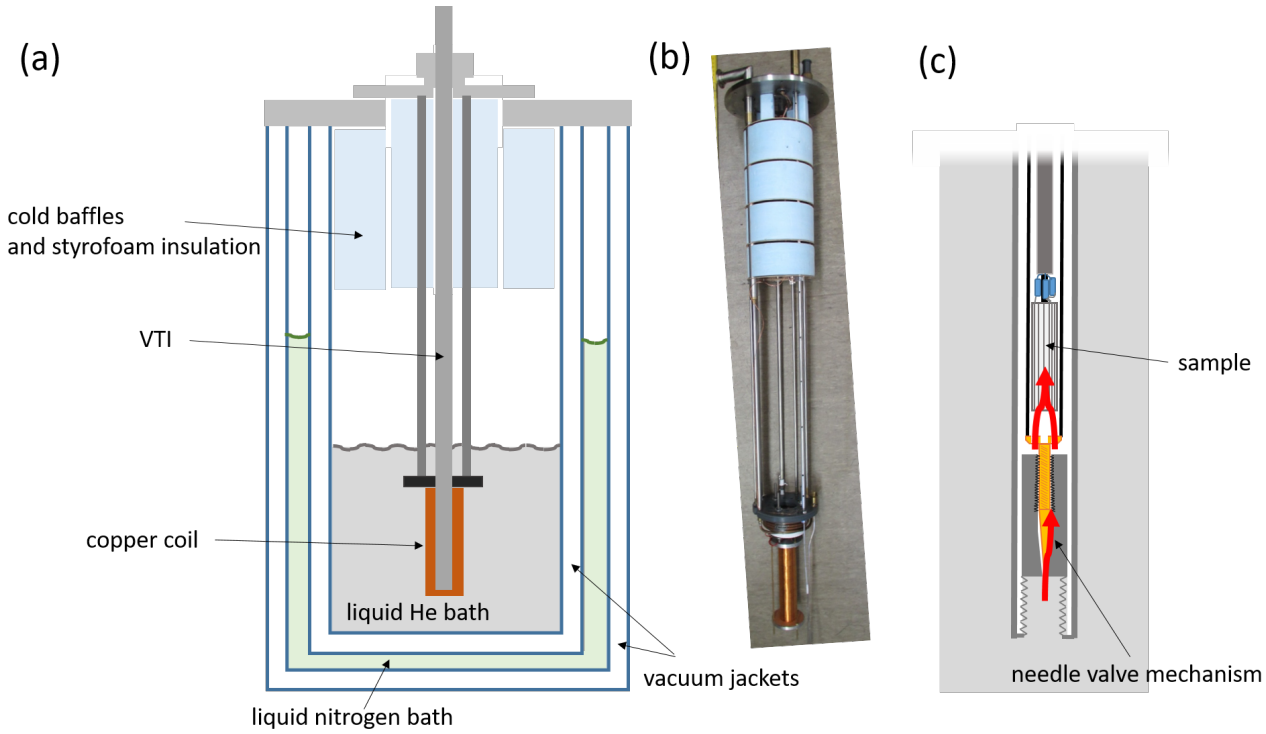

FIG. 10: Cryostat used in the experiment: (a) Sketch of the cryostat, (b) image of the VTI insert and mount including the copper coil, (c) needle valve mechanism and flow path of the liquid helium (red arrows) and sample position in the VTI.

[1] W. Buckel, Supraleitung: Grundlagen und Anwendungen, Physik Verlag, Weinheim/Bergstr., 1972.

[2] E.A. Lynton, Supraleitung, Bibliographisches Institut, Mannheim, 1966.

[3] Ch. Kittel, Introduction to Solid State Physics, John Wiley & Sons, Inc., New York, 1963.

[4] A.C. Rose-Innes & E.H. Rhoderick, Introduction to Superconductivity, Pergamon Press Ltd., 1969.

[5] D.J. Quinn and W.B. Ittner, J. Appl. Phys. 33, 748 (1962).

[6] W. Meissner and R. Ochsenfeld, Die Naturwissenschaften 21 (4), 787 (1933).

[7] J. D'Ans et E. Lax, Taschenbuch für Chemiker und Physiker, zweite, berichtigte Auflage, Springer Verlag, 1949.

[8] E. Maxwell, Phys. Rev. 78, 477 (1950).

[9] C.A. Reynolds et al., Phys. Rev. 78, 487, 1950; Phys. Rev. 84, 691 (1951).

[10] D.K. Finnemore and D.E. Mapother, Phys. Rev. Letters 9, 288 (1962).

[11] H. Rogalla, P.H. Kes, 100 Years of Superconductivity, CRC Press, 2012.

[12] W. Tuyn and H. Kamerlingh Onnes, THE DISTURBANCE OF SUPRA-CONDUCTIVITY BY MAGNETIC FIELDS AND CURRENTS. THE HYPOTHESIS OF SILSBEE., Journal of the Franklin Institute 201, 379 (1926).

[13] H.R. Betz, Staatsexamesarbeit: Planung und Aufbau eines Praktikumversuches zur Messung der kritischen Temperatur und des kritischen Magnetfeldes von Zinn beim Übergang in den supraleitenden Zustand, Universität Würzburg, 1973